

First Structural Characterization of a Delocalized, Mixed-Valent, Triangular Cu_3^{7+} Species: Chemical and Electrochemical Oxidation of a $\text{Cu}^{\text{II}}_3(\mu_3\text{-O})$ Pyrazolate and Electronic Structure of the Oxidation Product

Gellert Mezei,[†] John E. McGrady,^{*,‡} and Raphael G. Raptis^{*,†}

Department of Chemistry, University of Puerto Rico, San Juan, Puerto Rico 00931-3346, and Department of Chemistry, University of York, Heslington, York YO10 5DD, United Kingdom

Received May 9, 2005

The chemical or electrochemical one-electron oxidation of the all- Cu^{II} complex $[\text{Cu}_3(\mu_3\text{-O})(\mu\text{-pz})_3\text{X}_3]^{2-}$ leads to its formally $\text{Cu}^{\text{II}}_2\text{Cu}^{\text{III}}$ analogue (pz = pyrazolato anion; X = Cl^- and PhCOO^-). The X-ray single-crystal structure and density functional theory analysis of the latter agree in revealing the delocalized nature of its mixed-valent Cu_3^{7+} core.

Redox-active trinuclear copper clusters constitute the active centers of several copper proteins, such as ascorbate oxidase, laccase, and ceruloplasmin.¹ Particulate methane monooxygenase (pMMO) had also been suggested on the basis of spectroscopic data to contain tricopper active sites,² but a recent structure determination at 2.8-Å resolution of pMMO from *Methylococcus capsulatus* (Bath) has revealed dinuclear and remote mononuclear centers instead.³ The four-electron transfer required for the reduction of dioxygen to oxide by a tricopper center may involve either more than one trinuclear unit with Cu atoms cycling between the 1+ and 2+ oxidation states or a single unit cycling between Cu_3^{3+} and a mixed-valent Cu_3^{7+} state. While homovalent Cu_3^{3+} and Cu_3^{6+} , as well as mixed-valent Cu_3^{4+} and Cu_3^{5+} , complexes abound, there is only one example of a crystallographically characterized Cu_3^{7+} complex.⁴

We have recently described the synthesis and magnetic properties of a series of trinuclear $\text{Cu}^{\text{II}}_3(\mu_3\text{-E})$ (E = O and

OH) and $\text{Cu}^{\text{II}}_3(\mu_3\text{-E})_2$ (E = Cl and Br) clusters and shown that the sign and magnitude of magnetic exchange between the copper centers is strongly dependent on the Cu–E–Cu angle.^{5,6} In this paper, we turn our attention to their one-electron-oxidized, formally $\text{Cu}^{\text{II}}_2\text{Cu}^{\text{III}}$, analogues. We describe the electrochemical oxidation of $[\text{Cu}^{\text{II}}_3(\mu_3\text{-O})(\mu\text{-pz})_3\text{X}_3]^{2-}$ [pz = pyrazolate anion, $\text{C}_3\text{H}_3\text{N}_2^-$, and X = Cl^- (1^{2-}) and CF_3COO^- (2^{2-})] and the structural characterization of the one-electron-oxidized, mixed-valent species, 3^- (X = PhCOO^-), formed by chemical oxidation of $(\text{Bu}_4\text{N})_2[\text{Cu}^{\text{II}}_3(\mu_3\text{-Cl})_2(\mu\text{-pz})_3\text{Cl}_3]$ with AgO_2CPh . In addition, we use density functional theory to probe the changes in electron distribution associated with oxidation of the Cu_3^{6+} core to the mixed-valent Cu_3^{7+} form.

The cyclic voltammogram of 1^{2-} (4 mM in 0.5 M $\text{Bu}_4\text{-NPF}_6/\text{CH}_2\text{Cl}_2$, Pt working electrode, 295 K) in the potential range -1.00 to $+1.20$ V (vs Fc/Fc⁺) shows a reversible one-electron oxidation centered at -0.013 V; no other electrode process is observed up to the solvent oxidation limit. Under the same conditions, the reversible oxidation of 2^{2-} occurs at 0.131 V.⁷ Similar electrochemical results have been reported for some trinuclear oximate complexes.⁸ Oxidation of a green CH_2Cl_2 solution of 1^{2-} ($\lambda_{\text{max}} = 14\,900\text{ cm}^{-1}$)⁵ with a stoichiometric amount of $(\text{PhCO}_2)_2$ gave a reddish-

* To whom correspondence should be addressed. E-mail: jem15@york.ac.uk (J.E.M.), raphael@adam.uprr.pr (R.G.R.).

[†] University of Puerto Rico.

[‡] University of York.

- (1) Solomon, E. I.; Sundaram, U. M.; Machonkin, T. E. *Chem. Rev.* **1996**, *96*, 2563.
- (2) (a) Nguyen, H.-H. T.; Nakagawa, K. H.; Hedman, B.; Elliott, S. J.; Lidstrom, M. E.; Hodgson, K. O.; Chan, S. I. *J. Am. Chem. Soc.* **1996**, *118*, 12766. (b) Lieberman, R. L.; Rosenzweig, A. C. *Crit. Rev. Biochem. Mol. Biol.* **2004**, *39*, 147.
- (3) (a) Lieberman, R. L.; Rosenzweig, A. C. *Nature* **2005**, *434*, 177. (b) Sommerhalter, M.; Lieberman, R. L.; Rosenzweig, A. C. *Inorg. Chem.* **2005**, *44*, 770.
- (4) (a) Cole, A. P.; Root, D. E.; Mukherjee, P.; Solomon, E. I.; Stack, T. D. P. *Science* **1996**, *273*, 1848. (b) Root, D. E.; Henson, M. J.; Machonkin, T.; Mukherjee, P.; Stack, T. D. P.; Solomon, E. I. *J. Am. Chem. Soc.* **1998**, *120*, 4982. (c) Yoon, J.; Mirica, L. M.; Stack, T. D. P.; Solomon, E. I. *J. Am. Chem. Soc.* **2004**, *126*, 12586.

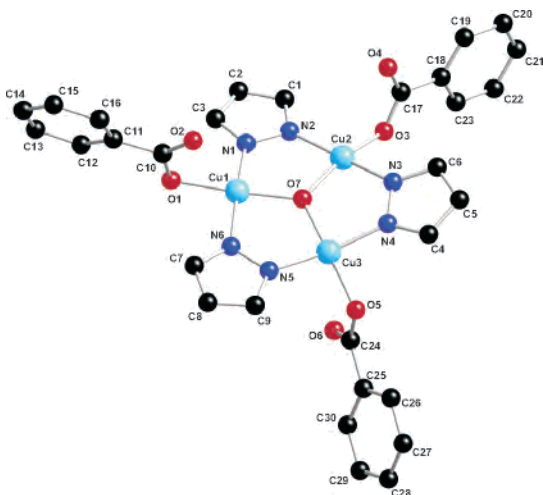
(5) Angaridis, P. A.; Baran, P.; Boca, R.; Cervantes-Lee, F.; Haase, W.; Mezei, G.; Raptis, R. G.; Werner, R. *Inorg. Chem.* **2002**, *41*, 2219.

(6) Boca, R.; Dihan, L.; Mezei, G.; Ortiz-Pérez, T.; Raptis, R. G.; Telser, J. *Inorg. Chem.* **2003**, *42*, 5801.

(7) Synthesis of $(\text{PPN})_2[2^{2-}]$: To a solution of $(\text{PPN})_2[1^{2-}]$ (300 mg, 0.19 mmol) in 6 mL of CH_2Cl_2 was added $\text{F}_3\text{CCO}_2\text{Ag}$ (125 mg, 0.57 mmol), and the resulting solution was stirred for 24 h in the dark. AgCl was filtered out, and the product was crystallized by Et_2O vapor diffusion into the filtrate. Yield: 245 mg (71%). Mp: 181–182 °C. Calculated/found (%): C, 57.28/56.83; H, 3.82/3.94; N, 6.14/6.16. IR (KBr pellet, cm^{-1}): 1697s (ν_{as} , COO), 836w, 1132s, and 1201s (CF_3 vibr). $^1\text{H NMR}$ (CDCl_3 , ppm): 35.56 (s, $w_{1/2} = 78$ Hz, 2H), 39.08 (s, $w_{1/2} = 54$ Hz, 1H). X-ray data for $(\text{PPN})_2[2^{2-}]$: $(\text{C}_{51}\text{H}_{39}\text{Cu}_3\text{F}_9\text{N}_7\text{O}_7\text{P}_2)$, $M_r = 1285.48$, triclinic, space group $P1$ (No. 2), $a = 16.047(2)$ Å, $b = 22.287(3)$ Å, $c = 27.400(3)$ Å, $\alpha = 66.65(1)^\circ$, $\beta = 89.78(1)^\circ$, $\gamma = 89.946(9)^\circ$, $V = 8992(2)$ Å³, $Z = 2$. Because of severe crystallographic disorder of all three CF_3COO groups, refinement to “acceptable for publication” values was not successful. However, the nature of the complex and the positions of all non- CF_3COO atoms were unequivocally determined.

Table 1. Selected Crystallographically Determined and Calculated Bond Lengths

		1^{2-} (X = Cl)	1^{-} (X = Cl)	3^{2-} (X = OCOPh)	3^{-} (X = OCOPh)
X-ray	Cu–(μ_3 -O)	1.890(2)–1.893(3) ^a			1.880(3)–1.896(4)
	Cu–Cu	3.269(1)–3.287(1) ^a			3.245(1)–3.283(1)
	Cu–N	1.946(3)–1.958(3) ^a			1.885(5)–1.901(5)
	Cu–X	2.295(1)–2.298(2) ^a			1.933(4)–1.947(4)
calcd	Cu–(μ_3 -O)	1.92–1.93	1.91–1.92	1.91–1.92	1.90–1.91
	Cu–Cu	3.33–3.35	3.31–3.32	3.29–3.33	3.29–3.30
	Cu–N	1.99–2.00	1.93–1.94	2.00–2.01	1.93
	Cu–X	2.44–2.45	2.34	2.09–2.11	2.02

^a Reference 5.**Figure 1.** Ball-and-stick diagram of 3^{-} . Selected distances (Å) and angles (deg): Cu···Cu = 3.245(1), 3.262(1), and 3.283(1); Cu–(μ_3 -O) = 1.881(3), 1.896(4), 1.880(3); Cu–N = 1.891(5), 1.901(5), 1.886(4), 1.896(5), 1.885(5), 1.886(5); Cu–O = 1.935(4), 1.947(4), 1.933(4); Cu–(μ_3 -O)–Cu = 120.3(2), 118.4(2), 120.7(2); N–Cu–N = 170.3(2), 173.9(2), 165.3(2).

brown solution of 1^{-} ($\lambda_{\max} = 9530$ and $22\,530\text{ cm}^{-1}$), which rapidly decomposes back to 1^{2-} . Although we have so far been unable to isolate the oxidized products, 1^{-} and 2^{-} , a few reddish-brown crystals of their isovalent species (Bu_4N)[3^{-}] were serendipitously obtained from the reaction of 1^{2-} with AgO_2CPh in CH_2Cl_2 (a silver mirror also resulted).⁹ The structure of 3^{-} consists of a $\text{Cu}_3(\mu_3\text{-O})$ core supported by bridging pyrazolate ligands, while terminal benzoates complete the approximately square-planar coordination of the Cu atoms (Figure 1). The $\text{Cu}_3(\mu_3\text{-O})$ core is rather similar to that in 1^{2-} , with approximately trigonal-

planar coordination about O7 (O7 is 0.0815 \AA out of the Cu_3 plane) and Cu–O7–Cu angles of $118.44\text{--}120.73^\circ$. The $[\text{Cu}(\mu\text{-pz})_3]$ frame of 3^{-} is also distorted in a similar way to 1^{2-} , but to a lesser extent, with one pyrazole rotated out of the Cu_3O plane (5.8°) and the other two bent by 14.5 and 22.3° out and on either side of this plane. The Cu–Cu distances, averaging $3.263(1)\text{ \AA}$, are similar to those in 1^{2-} [$3.269(1)$ and $3.287(1)\text{ \AA}$], as are the average Cu–(μ_3 -O) bond lengths: $1.886(3)\text{ \AA}$ in 3^{-} and $1.891(2)\text{ \AA}$ in 1^{2-} . The Cu–N bond lengths of 3^{-} [average: $1.891(5)\text{ \AA}$], in contrast, are considerably shorter than those in 1^{2-} [average: $1.952(3)\text{ \AA}$]. Perhaps the most striking feature of the $\text{Cu}_3(\mu_3\text{-O})$ core is its nearly perfect 3-fold symmetry, which suggests a delocalized electron distribution. This observation stands in stark contrast to the $[\text{Cu}_3(\mu_3\text{-O})_2\text{X}_3]^{3+}$ species [X = N-permethylated (1*R*,2*R*)-cyclohexanediamine] reported by Stack and co-workers, where the presence of two long (1.98 and 2.01 \AA) and one short (1.83 \AA) Cu–(μ_3 -O) bonds provided clear evidence for a localized $\text{Cu}^{\text{II}}_2\text{Cu}^{\text{III}}$ core.^{4b}

The optimized structural parameters¹⁰ of 1^{n-} and 3^{n-} ($n = 1$ and 2) are collected in Table 1 along with the corresponding experimentally determined ones. For the homovalent Cu^{II}_3 species ($n = 2$), the optimized ground state is a C_2 -symmetric doublet ($S = 1/2$), although a C_s -symmetric structure, differing only in the orientation of the pyrazole rings, has been located only 0.4 kcal mol^{-1} higher in energy. The $\text{Cu}_3(\mu_3\text{-O})$ cores are almost identical for the two structures, suggesting that the “flapping” of the pyrazole rings is a relatively facile process, consistent with their magnetic equivalence in solution.⁵ In the case of 1^{2-} , the calculated bond lengths and angles are in good agreement with their crystallographic counterparts, with the Cu–X and Cu···Cu distances being overestimated by approximately 0.05 \AA . The frontier orbitals of 1^{2-} (those of 3^{2-} are essentially identical), summarized in Figure 2a, clearly support the antiferromagnetic coupling proposed for this species.⁵ The two spin- α electrons are localized on the copper centers linked by the principal axis (spin densities $+0.33$), while the spin- β electron is localized on the unique copper center lying on

(8) (a) Chakravorty, A.; Mascharak, P. K.; Datta, D. *Inorg. Chim. Acta* **1978**, *27*, L95. (b) Datta, D.; Mascharak, P. K.; Chakravorty, A. *Inorg. Chem.* **1981**, *20*, 1673. (c) Datta, D.; Chakravorty, A. *Inorg. Chem.* **1982**, *21*, 363. (d) Datta, D.; Chakravorty, A. *Inorg. Chem.* **1983**, *22*, 1611.

(9) X-ray diffraction data were collected with a Bruker AXS SMART 1K CCD diffractometer, graphite-monochromated Mo $K\alpha$ radiation at 298 K , corrected for Lorentz and polarization effects. Structure solution by direct methods and refinement by full-matrix least-squares refinement based on F^2 . For $(\text{Bu}_4\text{N})[3^{-}]$ ($\text{C}_{46}\text{H}_{60}\text{Cu}_3\text{N}_7\text{O}_7$): $M_r = 1013.63$, orthorhombic, space group *Pbca* (No. 61), $a = 21.503(3)\text{ \AA}$, $b = 18.071(3)\text{ \AA}$, $c = 25.455(4)\text{ \AA}$, $V = 9892(3)\text{ \AA}^3$, $Z = 8$, $\rho_{\text{calc}} = 1.361\text{ g/cm}^3$, $2\theta_{\text{max}} = 46.62^\circ$, 41 688 reflections collected (7131 independent, $R(\text{int}) = 0.0857$), $R1 = 0.0452$ and $wR2 = 0.1097$ for 3475 reflections with $I > 2\sigma(I)$ (0.1156 and 0.1357 for all data) and 572 parameters. The crystallographic disorder of the Bu_4N^+ ions was not modeled. IR spectrum (cm^{-1} , KBr disks) of $(\text{Bu}_4\text{N})[3^{-}]$: 624w , 683m , 720m , 763m , 842w , 1025w , 1064m , 1132w , 1172w , 1192w , 1294m , 1348s , 1373m , 1429w , 1448w , 1485w , 1572m , 1612m , 2874w , 2932w , 2961w .

(10) All calculations were performed using the Gaussian 98 programme¹¹ with the Becke3LYP functional¹² and the lan12dz basis set on Cu, 6-31G(d,p) on all atoms directly bonded to Cu (O, N, and Cl) and 3-21G on all remaining atoms. The hybrid QM/MM approach was used for the OCOPh ligands, where OCOPh (carboxylate) was included in the QM partition and the phenyl group in the MM partition. The identity of all minima was confirmed by vibrational analysis [for the OCOPh systems, three residual imaginary frequencies ($< -15\text{ cm}^{-1}$ in all cases) associated with rotations of the Ph groups remained after optimization].

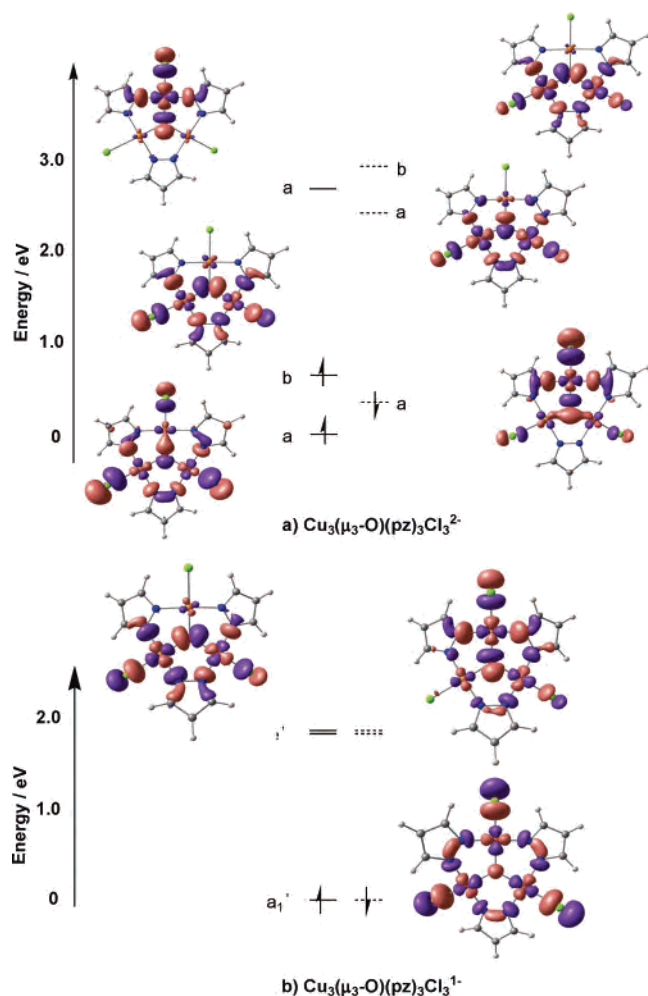


Figure 2. Frontier molecular orbital arrays for (a) $[\text{Cu}_3(\mu_3\text{-O})(\mu\text{-pz})_3\text{Cl}_3]^{2-}$ ($\mathbf{1}^{2-}$) and (b) $[\text{Cu}_3(\mu_3\text{-O})(\mu\text{-pz})_3\text{Cl}_3]^{1-}$ ($\mathbf{1}^{-}$). Orbitals are labeled according to the local C_2 ($\mathbf{1}^{2-}$) and D_{3h} ($\mathbf{1}^{-}$) symmetry of the $\text{Cu}_3(\mu\text{-O})$ core.

the axis (spin density -0.21). The corresponding ferromagnetically coupled state ($S = 3/2$) lies 0.23 eV higher in energy, consistent with the reported strong antiferromagnetic coupling ($J_{\text{Cu-Cu}} = -500 \text{ cm}^{-1}$).⁵

Oxidation to the mixed-valent state ($n = 1$) generates a singlet ground state, where the $\text{Cu}_3(\mu_3\text{-O})$ core again has almost perfect 3-fold rotational symmetry. Significantly, the structural changes accompanying oxidation are similar for both systems ($X = \text{Cl}^-$ and PhCOO^-), confirming that the crystallographic differences between $\mathbf{1}^{2-}$ and $\mathbf{3}^-$ reflect the intrinsic electronic effects of oxidation rather than the change in terminal ligands. Consistent with the experiment, the Cu–O and Cu–Cu distances are essentially unaffected by the oxidation process, while the Cu–N and Cu–X bonds contract by $0.06\text{--}0.10$ Å. The singlet ground state (Figure 2b) shows no open-shell character, and the copper-based electrons are delocalized over all three metal centers, in complete contrast to the localized electronic structure described by Stack, Solomon, and co-workers for the isovalent $\text{Cu}_3(\mu_3\text{-O})_2$ core.^{4b} The dramatic differences be-

tween the two systems can be traced to the nature of the interactions between the Cu $d_{x^2-y^2}$ orbitals and the p orbitals on the oxide ligands. In the limit of local D_{3h} symmetry, the $d_{x^2-y^2}$ orbitals in the trigonal-bipyramidal $\text{Cu}_3(\mu_3\text{-O})_2$ core, which lie *perpendicular to the Cu_3 plane*, form linear combinations of a_1'' and e'' symmetry. Both a_1'' and e'' are destabilized by interactions with the 2p orbitals on the oxide ligands.^{4b,13} As a result, the splitting within the Cu $d_{x^2-y^2}$ manifold is relatively small (~ 0.5 eV), and an orbitally degenerate triplet ground state (${}^3E'$) emerges. Coupling of this degenerate electronic state to a vibrational mode of the same symmetry leads to a strong Jahn–Teller distortion and, hence, to a localized $\text{Cu}^{\text{III}}\text{Cu}^{\text{II}}_2$ ground state.¹³ In contrast, the nearly perfect D_{3h} symmetry of the planar $\text{Cu}_3(\mu_3\text{-O})$ core in $\mathbf{3}^-$ generates linear combinations of Cu $d_{x^2-y^2}$, which lie *in the Cu_3 plane*, with a_1' and e' symmetry, but only the latter has the correct symmetry to interact with 2p orbitals on the oxide ligand. The totally symmetric combination is destabilized to a much lesser extent by interactions with the oxide 2s orbital, as a result of which the splitting within the manifold is much larger (1.85 eV), leading to an orbitally nondegenerate singlet state (${}^1A_1'$). The absence of a Jahn–Teller instability in this case means that there is no driving force for the localization of the valence electrons similar to that observed in the $\text{Cu}_3(\mu_3\text{-O})_2$ case.

In conclusion, we have shown that the supporting ligand topology is the critical factor in determining the electronic structure of mixed-valent tricopper complexes. The delocalized Cu_3^{7+} core presents a new alternative to the electronic structure of this biologically relevant cluster.

Acknowledgment. G.M. acknowledges an EPSCoR-NSF doctoral fellowship (Grant 9874782).

Supporting Information Available: Crystallographic data in CIF format (Table S1), ORTEP diagram (Figure S2), Cartesian coordinates and total energies of all optimized structures (Table S3), infrared spectrum for $\mathbf{3}^-$ (Figure S4), and cyclic voltammograms for $\mathbf{1}^{2-}$ and $\mathbf{2}^{2-}$ (Figure S5). This material is available free of charge via the Internet at <http://pubs.acs.org>.

IC050729E

- (11) Frisch, M. J.; Trucks, G. W.; Schlegel, H. B.; Scuseria, G. E.; Robb, M. A.; Cheeseman, J. R.; Zakrzewski, V. G.; Montgomery, J. A.; Stratmann, R. E.; Burant, J. C.; Dapprich, S.; Millam, J. M.; Daniels, A. D.; Kudin, K. N.; Strain, M. C.; Farkas, O.; Tomasi, J.; Barone, V.; Cossi, M.; Cammi, R.; Mennucci, B.; Pomelli, C.; Adamo, C.; Clifford, S.; Ochterski, J.; Petersson, G. A.; Ayala, P. Y.; Cui, Q.; Morokuma, K.; Malick, D. K.; Rabuck, A. D.; Raghavachari, K.; Foresman, J. B.; Cioslowski, J.; Ortiz, J. V.; Stefanov, B. B.; Liu, G.; Liashenko, A.; Piskorz, P.; Komaromi, I.; Gomperts, R.; Martin, R. L.; Fox, D. J.; Keith, T.; Al-Laham, M. A.; Peng, C. Y.; Nanayakkara, A.; Gonzalez, C.; Challacombe, M.; Gill, P. M. W.; Johnson, B. G.; Chen, W.; Wong, M. W.; Andres, J. L.; Head-Gordon, M.; Replogle, E. S.; Pople, J. A. *Gaussian 98*, revision A.7; Gaussian, Inc.: Pittsburgh, PA, 1998.
- (12) (a) Becke, A. D. *Phys. Rev. A* **1988**, *38*, 3098. (b) Lee, C.; Yang, W.; Parr, R. G. *Phys. Rev. B* **1988**, *37*, 785.
- (13) Daul, C.; Fernandez-Ceballos, S.; Ciofini, I.; Rauzy, C.; Schläpfer, C.-W. *Chem. Eur. J.* **2002**, *8*, 4392–4401.